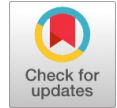# Crosstalk Characterization and Reduction in Power Lines

Jacquie Therese NGO BISSE, Bedel Giscard ONANA ESSAMA, Joseph KOKO KOKO, Jacques ATANGANA, Salomé NDJAKOMO ESSIANE

Abstract: We propose a technique of crosstalk reduction through power lines. This crosstalk reduction technique uses the pseudo-matched impedances' method that determines the characteristic parameters of the chosen line through the transmission lines' theory. Besides, we establish the telegrapher's equations to determine the characteristic impedances of the line. Further, two types of lines are employed here to apply the pseudo-matched impedances' method. The far-and near-ends crosstalk are measured with two strategies known as Simulink diagram and Matlab code. The Simulink diagram of the power line provides crosstalk curves and the Matlab code directly returns crosstalk values. It appears that the crosstalk has a reduction rate between 20 and 50% compared to previous investigations using pseudo-matched impedances in literature. Moreover, the variation of two different types of impedances leads to a crosstalk reduction rate that approaches 99%.

Keywords: Crosstalk, Far-End Crosstalk, Near-End Crosstalk, Pseudo Adapted Impedances, Electromagnetic Compatibility.

I. INTRODUCTION

The source can represent any device or physical-electrical phenomenon that induces electromagnetic disturbances by conduction or radiation. Among the main causes of disturbances, we can name the distribution of electrical energy, the propagation of radio waves, the electrostatic discharges, the electric motors, the lightning, etc. The crosstalk phenomenon stands for the interference induced by the electromagnetic waves that influence the electric signals sent through power network lines [1-5].

Dr. Jacquie Therese NGO BISSE[1], Email: jacquieday13@gmail.com
Dr. Bedel Giscard ONANA ESSAMA[2]*, Email: onanaessama@yahoo.fr,
ORCID ID: 0000-0002-9900-0419
Dr. Joseph KOKO KOKO[3], Email: kokojoseph469@yahoo.fr
Prof. Jacques ATANGANA[4], Email: acquesatangana215@yahoo.com
Prof. Salomé NDJAKOMO ESSIANE[5], Email: salomendjakomo@gmail.com
(1,2,3,5) Laboratory of Electrotechnics, Automatics and Energy, Department of Electrical Engineering, Higher Technical Teachers, Training College (HTTTC) of Ebolowa, University of Ebolowa, P.O. Box 886 Ebolowa, Cameroon
(1,2,5) Cameroonian Association for Research and Innovation in Environmental and Energetic Technologies (ACRITEE), P.O. Box, 59 Ebolowa, Cameroon
(4) Higher Teacher Training College of Yaounde, University of Yaounde I, P.O. Box 47 Yaounde, Cameroon.

Moreover, the crosstalk phenomenon also acts in optical transmission network cables. In this case, this phenomenon affects data communication in data centers, server rooms, and other areas where a constant flow of data is necessary. The crosstalk phenomenon is a common problem solved to provide the better networking and data transfer. Furthermore, there are two types of crosstalk phenomena which affect networks in various ways. Those crosstalk types are named near-end crosstalk and far-end crosstalk [1-5]. All the types of crosstalk are generated inductively (parasitic mutual inductance) or capacitively (parasitic mutual capacitance). Inductive crosstalk is only generated when the aggressor signal modifies the levels. Hence, higher speed signals generate stronger crosstalk. Besides, the capacitive crosstalk is generated by changing potential difference between the two interconnects [1-5]. In circuit models describing interconnects, the mutual inductance and capacitance are described the coupling between the aggressor and victim drivers [1-5].

There are several techniques to prevent and reduce the electromagnetic perturbations (crosstalk) so that they do not affect victim drivers. Among the victim drivers, we note two cases. The first one concerns the powered driver that receives an external disturbance. Besides, the second case, concerns the non-powered driver that receives an external disturbance. The investigation of this paper focuses on the last case [1-5].

Moreover, we precisely study the case of two drivers where the powered driver affects the non-powered one. This case is frequently observed in the interconnections of power transmission lines. Further, one question emerges: what can be done to reduce or delate this phenomenon? It is well known that to fight against those electromagnetic phenomena or radiation coupling, we can minimize ground loops, use shielding and/or move the victim receiver away from the source of disturbances [1-5]. Those techniques cannot provide a better solution to solve the crosstalk problem that occurs from the near field coupling in interconnected lines. Moreover, crosstalk phenomena have also been on other physical systems such as light waves networks [6-12], bus networks [13], and gene networks [14-19]. However, the use of pseudo-matched impedances' method to reduce and characterize the crosstalk phenomena in power lines, has been least reported in literature. The paper is organized as follows. In Sec. 2, Moreover, we establish the equations of the telegraphers to determine the characteristic parameters of the studied line. Then, we develop the pseudo-matched impedances' method and characterize the crosstalk phenomenon.

In Sec.3, we present the results and discussion of numerical simulations corresponding the crosstalk reduction on the line under consideration. Thereafter, the outcomes are compare to some results previously obtained in literature. In Sec.4, we summarize.

II. MATHEMATICAL DEVELOPMENT AND THE MODEL

We use the computer and the Matlab software as key tools to solve the crosstalk problem. The investigation includes both analytical and numerical aspects. The analytical aspect concerns the determination characteristic parameters related to the electric power transmission line. From those parameters, we establish the mathematical models including the voltage, the current and characteristic impedance matrices of the line. Those different matrices associated with pseudo adapted impedances are inserted at the ends of the lines. Further, the numerical aspect of this method concerns the simulation of a two-driver lines' model with pseudo-matched impedances. Those simulations will be done in the MATLAB 2018a environment.

A. Transmission Line Theory

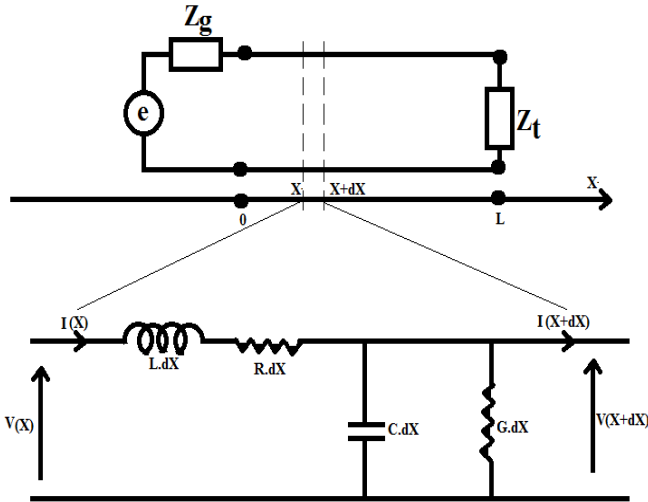We consider the diagram of Fig. (1) illustrating a model of transmission line [20].

Figure 1 – Model of Transmission Line Considered [20].

Considering the characteristic parameters of the circuit (R, L, C and G), and the second derivative, the telegraphers' equations are obtained as follows [20]:

$$-\frac{\partial^2 V}{\partial x^2} = LC.\frac{\partial^2 V}{\partial t^2} + (RC + LG).\frac{\partial V}{\partial t} + RG.V \quad (1)$$

$$-\frac{\partial^2 I}{\partial x^2} = LC.\frac{\partial^2 I}{\partial t^2} + (RC + LG).\frac{\partial I}{\partial t} + RG.I. \quad (2)$$

In sinusoidal regime and introducing the complex form, the telegraphers' equations become [20]:

$$-\frac{d^2 V}{dx^2} = ZY.V(x) \quad (3)$$

$$-\frac{d^2 I}{dx^2} = ZY.I(x) \quad (4)$$

with $Z = R + j\omega L$ and $Y = G + jC\omega$.

B. Pseudo-Matched Impedances' Method

This method consists to introduce impedances at the ends of the line to cancel the reflections when the pseudo-matched impedances are equivalent to the characteristic impedance of the line.

a. Characteristic Impedance of the Line

The matching network of a two-drivers' line has the role of absorbing the waves coming from the end where it is connected and not generating reflected waves.

To cancel the reflections occurring at the ends of the lines, a termination with an impedance matrix equal to the characteristic impedance matrix [Zc] of the CML is connected at each end of the line (see Fig. (2)).
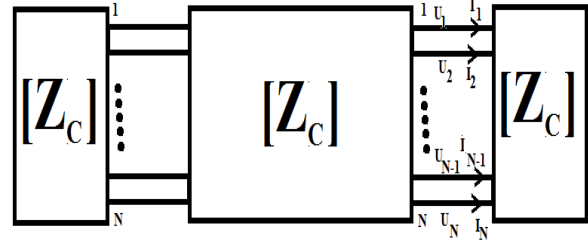

Figure 2. Illustration of MCL with Characteristic Impedance at the Ends [21].

Let us consider the case of a line with two drivers. This line is characterized by the following characteristic impedance matrix[21]:

$$[Zc] = \begin{bmatrix} Z_{C11} & Z_{C12} \\ Z_{C12} & Z_{C11} \end{bmatrix} \quad (5)$$

According to the definition of the matrix [Zc], it can verify the following equation [21]:

$$[U]=[Zc].[I] \quad (6)$$

where $[U] = \begin{bmatrix} U_1 \\ U_2 \end{bmatrix}$ et $[I] = \begin{bmatrix} I_1 \\ I_2 \end{bmatrix}$.

Combining Eqs. (7) and (8), we obtain Eqs. (9) and (10) as follows [21]:

$$U_1 = Z_{C11}.I_1 + Z_{C12}.I_2 \quad (7)$$

$$U_2 = Z_{C12}.I_1 + Z_{C11}.I_2. \quad (8)$$

We can therefore deduce the admittance expression as follows[21]:

$$Y_0 = [Zc]^{-1}. \quad (9)$$

The matrices [Z] and [Y] are frequency-dependent and defined from the matrices of the linear parameters of the line. In addition, we neglect R and G. So, we obtain [21]:

$$[Z] = j \cdot \omega \cdot [L] \quad (10)$$

$$[Y] = j \cdot \omega \cdot [C] \quad (11)$$

Equations (10) and (11) are obtained in the case of a lossless line.

2

b.   Modelling of Crosstalk Phenomenon

The illustration the crosstalk phenomenon is done by considering three drivers, impedances, and a power source as depicted in Fig. (3). We investigate in the case of a lossless line. The quantities V_{NE} (t) and V_{FE} (t) are induced voltages coming from the currents induced in the circuit. The term V_{NE} (t) corresponds to the near-end crosstalk and V_{FE} (t) stands for the far-end crosstalk. Thereafter, the pseudo-matched impedances are determined and are represented as follows:

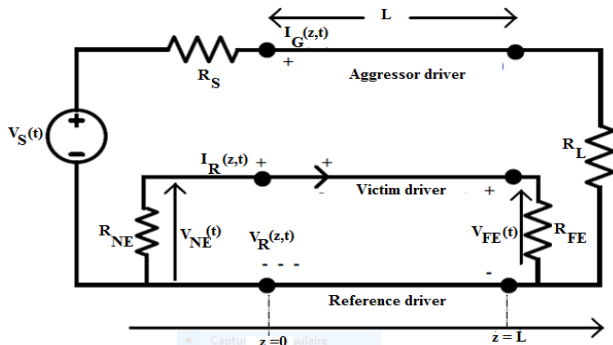$Z_c = R_S$; $Z_c = R_{NE}$; $Z_c = R_{NF}$; $Z_c = R_L$

Figure 3 - Unshielded Line Composed of three Drivers [21, 22].

c.   Initial conditions at the beginning of the simulation

Those conditions are presented in Table 1 as follows.

Table 1 - The Values of the Line Parameters

Lines				
Linear inductance (µH/m)	$L1=\begin{bmatrix}0.8629 & 0.3725\\0.3725 & 0.8629\end{bmatrix}$		$L2=\begin{bmatrix}0.9337 & 4.1264\\4.1264 & 0.9337\end{bmatrix}$	
Linear capacity (pF/m)	$C1=\begin{bmatrix}46.762 & -18.036\\-18.036 & 46.762\end{bmatrix}$		$C2=\begin{bmatrix}12.74 & 7.751\\7.751 & 12.74\end{bmatrix}$	
Impedance (ohm)	$Z_{C1}=\begin{bmatrix}147.1874 & 60.1923\\60.1923 & 147.1874\end{bmatrix}$		Zc2=444.1967	
Length (km)	d=100			
Number of drivers	N=2			
Sources				
Voltage(V)	U=250000			
Frequency (Hz)	f=50			
Phase shift (degree)	$\varphi = 15°; 30°; 60°; 90°$			

d.   Matlab Code

```
f=50;      (Frequency)
U=250000;   (voltage)
d=10000;     (length of propagation)
n=2;          (number of drivers)
l=[0.8629 0.3725; 0.3725 0.8629] ;  (Linear
inductance)
c=[46.762 -18.036; -18.036 46.762] ; (Linear
capacity)
L=l*d;
C=c*d;
w=2*pi*f;      (Angular frquency)
Zc=(L/C)^(1/2);  (characteristic impedance of the
line)
Y=w*C;          (line admittance )
Z=w*L;          (line impedance)
γ = √Z.Y        (Propagation coefficient)
Z1= Z2= Z3= Z4=Zc;
```

e.   Schematic Diagram

The schematic diagram is illustrated in Fig.(4) in Appendix. This Fig.(4) presents a multi-drivers' line (middle block) which is supplied with voltage from the first block on the left. The middle block is composed with three drivers, pseudo-matched impedances, current and voltage measuring devices. The last block on the right is used to observe the curves (see Fig.(4) in Appendix).

C.   The Model

a.   Electrical Diagram

The crosstalk phenomenon can be implemented in the MATLAB environment by the diagram depicted in Fig.(5).
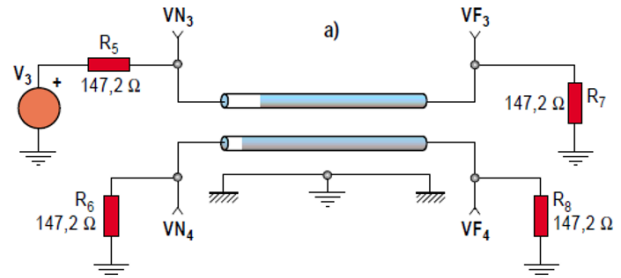

Figure 5- Network Configuration [23].

III.   RESULTS AND DISCUSSION

A.   Simulations using Matlab Code

The linear parameters provided in the mathematical development in Sec.2 are inserted in the Matlab code. A sinusoidal signal is injected on the line at the beginning of propagation. Therefore, the disturbed line obtained here, can allow the evaluation of the far-and near-ends crosstalk voltages on the second line (or victim driver).

a.   Results of Matlab Code

We use the line parameters presented in table 1 to the Matlab code exhibited in Sec. 2.2.4. Then, the results are listed in Table 2.

Table 2- Results Obtained with Two Types of Lines

Z_C= 147.1874 ohms			
Near-End crosstalk	Far-End crosstalk	Phase shift (°)	Reduction rate
8.09kV	0V	30	**100%**
24.92kv	0V	60	
29KV	0V	90	
Zc=444.1967 ohms			
Near-End - crosstalk	Far-End - crosstalk	Phase shift (°)	Reduction rate
15.182KV	0V	30	**100%**
26.296kv	0V	60	
30.364KV	0V	90	

We have here an overview of the results of Near-end-crosstalk and Far-end -crosstalk in this table

B.   Configuration of the Power Line

a.   Configuration of the First Power Line for the Zc1 Impedance

Initially, we use the setup in Fig. (5) to characterize the crosstalk with the pseudo-matched impedances of 147.2 Ω. Thereafter, we can observe the manifestation of crosstalk.

Besides, the far-and near-ends crosstalk will be respectively measured at the points V_{N4} and V_{F4}. Besides, another measurement can be directly done through Fig. (6) illustrated in Appendix.

b.   Configuration of the Second Line with Zc2 Impedance

The value of the impedance is changed as Zc2=444.196 Ω and we inject a new signal on the line. In the second configuration, the new impedance will allow us to check if our method effectively reduces or delates the crosstalk phenomenon on the line. Each impedance must be connected to the end of the line under consideration.

c.   Study Principle

The studied structure is supplied with a voltage source using constant amplitude and frequency. Then, we measure the induced voltage on the neighboring line (victim driver). The measurement of the crosstalk is done at the V_{NE} point (see Fig. (3)), using the scope when the line is powered by a voltage of 250Kv. The same source is applied in simulation under MATLAB at the frequency is 50Hz.

C.   Impact of Phase Shift on the Crosstalk Phenomenon

a.   Crosstalk Phenomenon on a Line with Zc=147.1874 ohms and φ=15°.

We obtain Fig. (7) for Zc=147.1874 ohms and φ=15°. The voltage injected in the line is depicted in Fig. 7(a). The injected voltage has a sinusoidal form with T=0.02 s as period. The amplitude of this injected curve is $1.25×10^5$ v as depicted in Fig. 7(a). Besides, the introduction of the near-end crosstalk reduces the voltage amplitude from $1.25×10^5$ v to $2.50×10^4$ v as illustrated in Fig. 7(a) and (b). The beginning of the propagation is moved from 0 v to $1.00×10^4$ v as seen in Fig. 7(a) and (b). Further, a fluctuation corresponding to a broken point appears at the beginning of the propagation at $T=0.6×10^{-3}$ s as depicted in Fig. 7(b). Moreover, the fluctuation has a horizontal and constant behavior when $0<T<0.6×10^{-3}$ s. This behavior becomes vertical and constant at $T=0.6×10^{-3}$ s when the amplitude varies between $0.6×10^4$ v and $1.0×10^4$ v as depicted in Fig. 7(b). Thereafter, the behavior of the voltage changes form vertical and constant to sinusoidal form for $T>0.6×10^{-3}$ s as depicted in Fig. 7(b). It appears that the behavior exhibited in Fig. 7(b) corresponds to the main behavior of the near crosstalk when Zc=147.1874 ohms and φ=15°. The near-end crosstalk value is $1.0×10^4$ v=10 Kv as depicted in Fig. 7(b).

The introduction of the far-end crosstalk changes the nature of the broken point as seen in Fig. 7(c). Besides, the voltage curve exhibits an ascendant and linear behavior when $0<T<0.6×10^{-3}$ s. This behavior changes from ascendant and linear to vertical and constant when $T=0.6×10^{-3}$ s as illustrated in Fig. 7(c). Moreover, the vertical and constant behavior of the voltage varies between 0 v and 520 v as depicted in Fig. 7(c). Furthermore, the voltage behavior changes again from the vertical and constant to horizontal and constant when $T>0.6×10^{-3}$ s as seen in Fig. 7(c). It appears that the strange behavior described in Fig 7(c) constitutes the main behavior of the far-end crosstalk when Zc=147.1874 ohms and φ=15°. The far-end crosstalk value is 520 v =0.52 Kv as depicted in Fig. 7(c).

b.   Crosstalk Phenomenon with Zc=147.1874 ohms and φ=30°.

The impedance is maintained at Zc=147.1874 ohms and the phase shift increases from φ=15° to φ=30°. The growth of the phase shift modifies the form of the injected curve from the sinusoidal form to the linear form as depicted in Figs. 7(a) and 8(a). Besides, the linear and ascendant behavior of the voltage curve undergoes a broken point at $T=0.6×10^{-3}$ s. Furthermore, this linear form varies between $-0.2×10^4$ v and $3.8×10^4$ v as depicted in Fig. 8(a).

The introduction of near-end crosstalk leads to Fig. 8(b). The precedent sinusoidal voltage associated with a small fluctuation seen in Fig. 7(b) is changed into the huge broken structure depicted in Fig. 8(b). The previous small broken point that appears in the linear source voltage in Fig. 8(a) has significantly increased as observed in Fig. 8(b). In fact, the near-end crosstalk curve progressively increases (ascendant behavior) from 9500 v to 9800 v when $0<T<0.6×10^{-3}$ s as illustrated in Fig. 8(b). Thereafter, we observe a vertical and constant decrease from 9800 v to 5000 v when $T=0.6×10^{-3}$ s. Then, the curve undergoes a brutal and linear increase (ascendant behavior) from 5000 v to 8000 v when $T>0.6×10^{-3}$ s as depicted in Fig. 8(b).
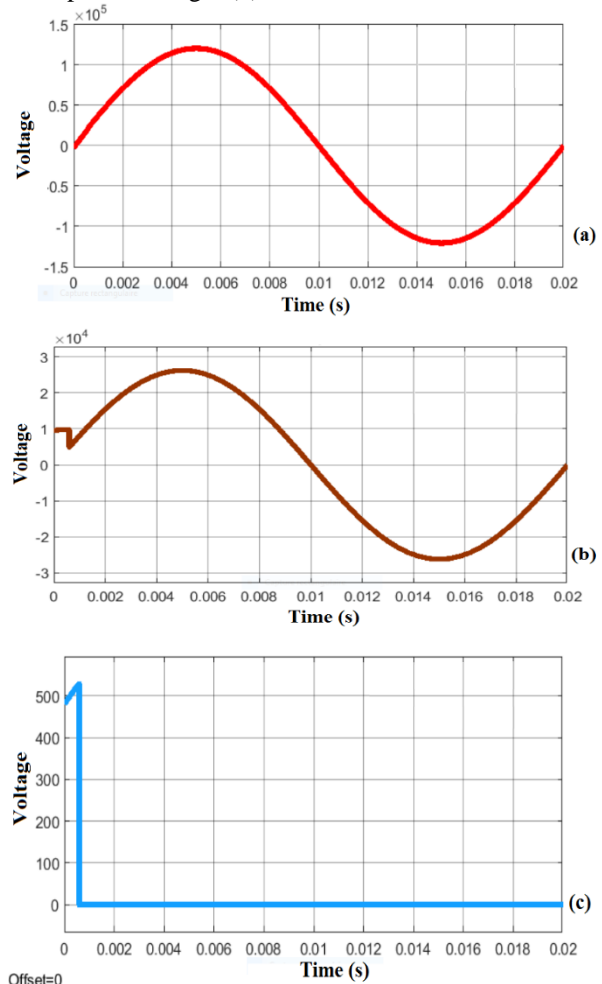
Figure 7: Crosstalk Curves for z=147.182 ohms and φ=15°: (a) Source Voltage; (b) Near-End Crosstalk; (c) Far-end Crosstalk.

The introduction of the far-end crosstalk leads to Fig. 8(c) where the huge broken structure still appears. However, the voltage values have significantly decreased. In fact, the far-end crosstalk curve gradually increases (ascendant behavior) from 4900 v to 5300 v when $0<T<0.6\times10^{-3}$ s as depicted in Fig. 8(c). Thereafter, we observe a vertical and constant decrease (linear form) from 5300 v to 0 v when $T=0.6\times10^{-3}$ s. Besides, the curve undergoes a constant and horizontal behavior (linear form) closed to 0 v when $T>0.6\times10^{-3}$ s as presented in Fig. 8(c).

It appears that the near-and far-ends crosstalk exhibit the same behaviors (Huge broken structure) when the phase shift is fixed to $\varphi=30°$. However, the voltage values associated to each effect are different as seen in Figs. 8(b) and (c). Consequently, the introduction of crosstalk phenomenon significantly, decreases the voltage values.
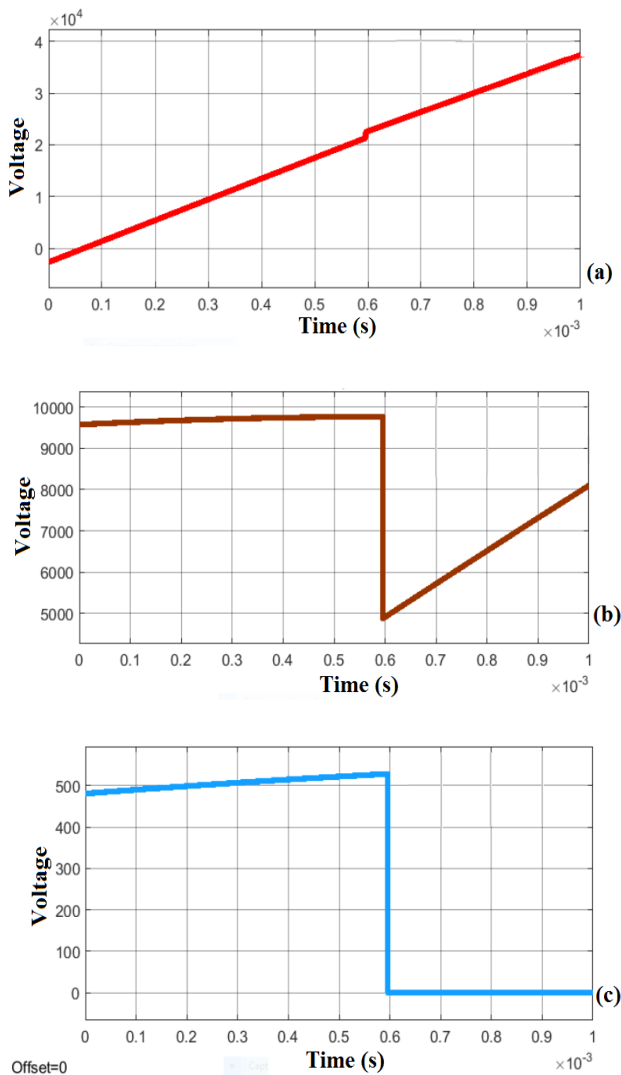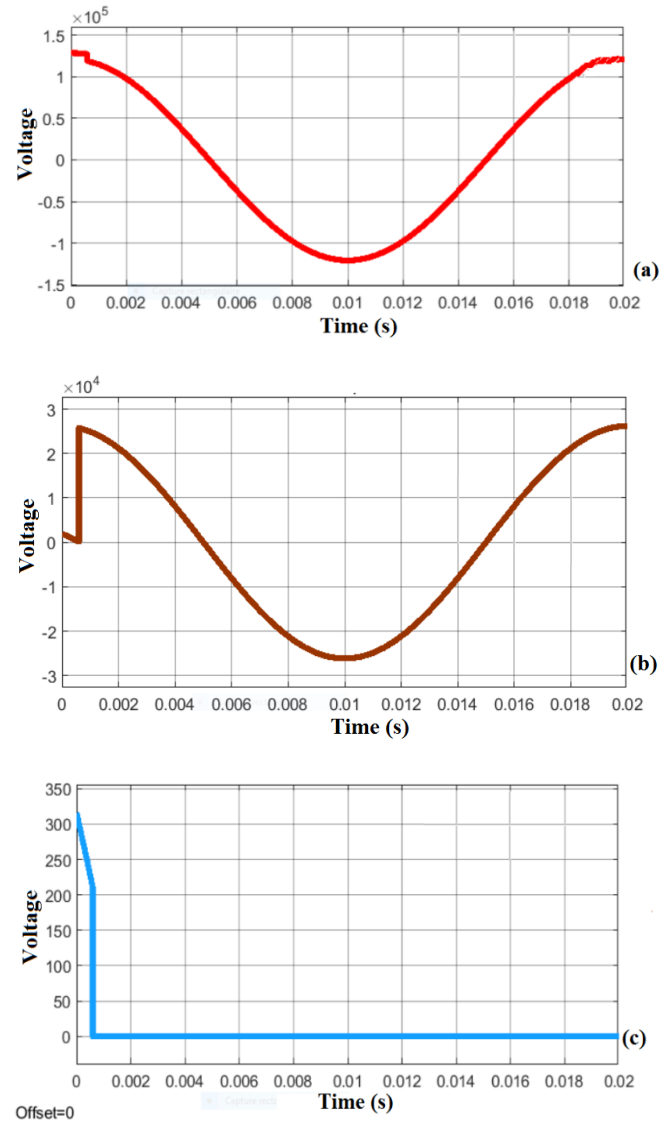

Figure 8- Crosstalk Curves for z=147.182 ohms and φ=30°: (a) Source Voltage(b) Near-End Crosstalk; (c) Far-End Crosstalk.

It appears the increase of the phase shift significantly modifies the impact of crosstalk phenomenon on the source voltage as illustrated in Figs. (7) and (8).

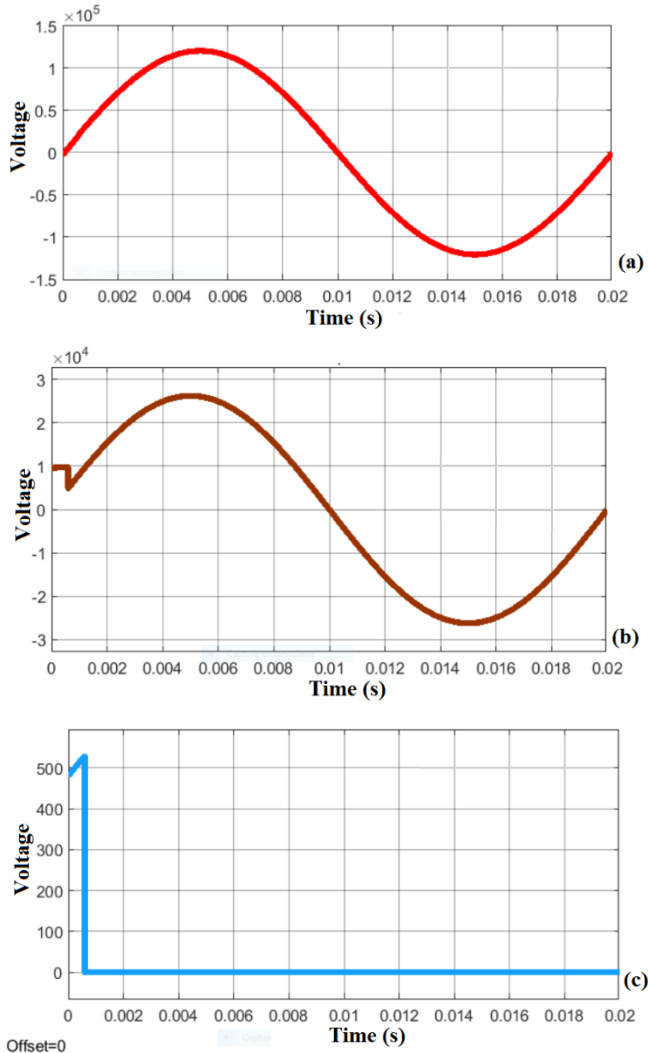*c.*   *Crosstalk Phenomenon with Zc=147.1874 ohms and φ=60°.*

The impedance is maintained to Zc=147.1874 ohms and the phase shift is increased from $\varphi=30°$ to $\varphi=60°$. Then, we obtain Fig. (9). The source voltage has changed its aspect from the precedent linear form depicted in Fig. 8(a) to the sinusoidal form illustrated in Fig. 9(a). This sinusoidal curve presents a small fluctuation at the beginning of the wave propagation at $T=0.5\times10^{-3}$ s as seen in Fig. 9(a).

Figure 9- Crostalk Curves for z=147.182 ohms and φ=60°: (a) Source Voltage; (b) Near-End Crosstalk; (c) Far-End Crosstalk.

The introduction of near-end crosstalk induces a huge broken point at the beginning of the propagation as seen in Fig. 9(b). The near-end crosstalk curve undergoes a small linear decrease (descendant behavior) form 0.2×10^{4} v to 0 v when $0<T<0.5\times10^{-3}$ s. Then, the curve exhibits a brutal vertical and constant increase from 0 v to 2.7×10^{4} v when $T=0.5\times10^{-3}$ s as illustrated in Fig. 9(b). More so, the curve maintains its sinusoidal aspect when $T=0.5\times10^{-3}$s as illustrated in Fig. 9(b).

The introduction of the far-end crosstalk totally destroyed the precedent sinusoidal form into a strange broken form as depicted in Figs. 9(b) and (c). The new form exhibits many steps. The curve presents a linear decrease from 320 v to 210 v when $0<T<0.5\times10^{-3}$ s as seen in Fig. 9(c). Besides, the curve undergoes a vertical and constant behavior from 210 v to 0 v when $T=0.5\times10^{-3}$ s. Further, the curve presents a constant and horizontal behavior closed to 0 v when $T>0.5\times10^{-3}$ s as seen in Fig. 9(c).
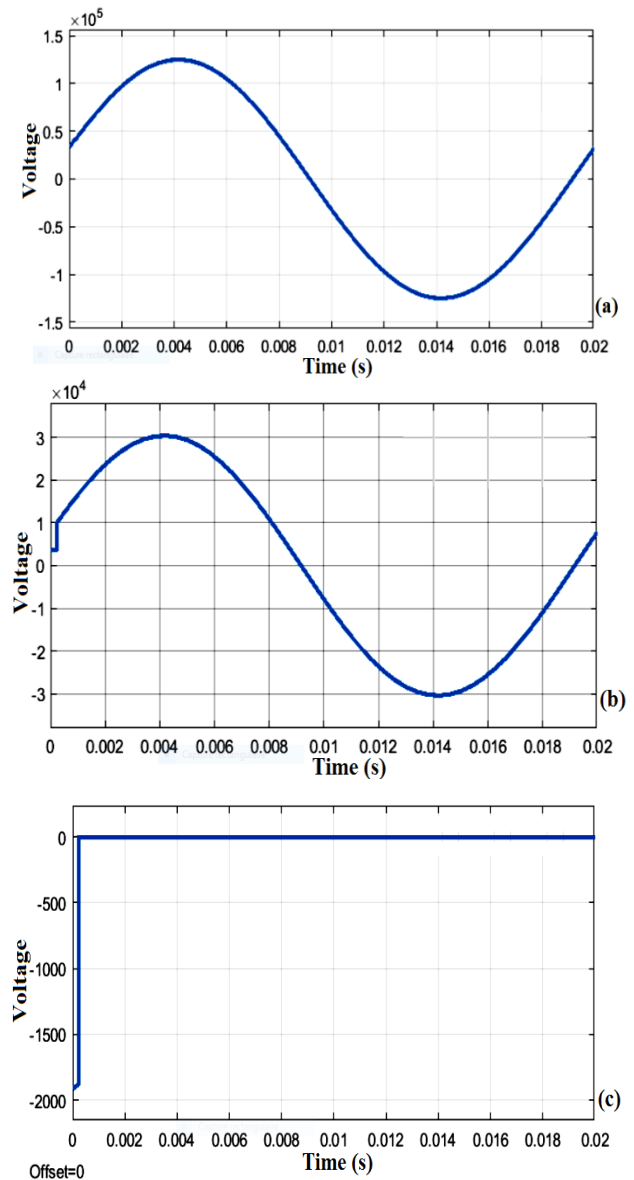

Figure 10- Crosstalk Curves for z=147.182 ohms and φ=90°: (a) Source Voltage; (b) Near-End Crosstalk; (c) Far-End Crosstalk.

d. Crosstalk Phenomenon with Zc=147.1874 ohms and φ=90°.

The impendance is maintained to Zc=147.1874 ohms and the phase shift increases from φ=60° to φ=90°. Then, Fig. (10) is obtained. The source voltage safeguards its sinusoidal form associated with an amplitude which approaches 1.25×10^5 v as depicted in Fig. 10(a). However, the introduction of the near-end crosstalk induces a decrease of amplitude from 1.25×10^5 v to 2.70×10^4 v as illustrated in Figs. 10(a) and (b). Moreover, a small fluctuation is also observed at the beginning of propagation as seen in Fig. 10 (b). Besides, the near-end crosstalk curve undergoes a constant and horizontal behavior (linear form) with an amplitude of 1.00×10^4 v when $0<T<0.5\times10^{-3}$ s as depicted in Fig. 10(b). Thereafter, the curve exhibits a vertical and constant behavior leading to the

decrease of the voltage from 1.00×10^4 v to 0.50×10^4 v when $T=0.5\times10^{-3}$s as depicted in Fig. 10(b). Further, the sinusoidal form is maintained when $T>0.5\times10^{-3}$s as seen in Fig. 10(b).

Figure 11 - Crosstalk Curves for z=444.196 ohms and φ=15°: (a) Source Voltage; (b) Near-End Crosstalk; (c) Far-End Crosstalk.

The introduction of the far-end crosstalk modifies the nature of the broken point as seen in Fig. 10(c). Besides, the voltage curve exhibits an ascendant and linear behavior from 500 v to 520 v when $0<T<0.5\times10^{-3}$ s. This behavior changes from ascendant and linear to vertical and constant when $T=0.5\times10^{-3}$ s as illustrated in Fig. 10(c). Moreover, the vertical and constant behavior of the voltage decreases from 520 v to 0 v as depicted in Fig. 10(c). Furthermore, the voltage behavior changes again from the vertical and constant to horizontal and constant when $T>0.5\times10^{-3}$ s as seen in Fig. 10(c). It appears that the crosstalk phenomenon modifies the system at the same way for two different values of phase shift (φ=15° and φ=90°) as depicted in Figs. (7) and (10).
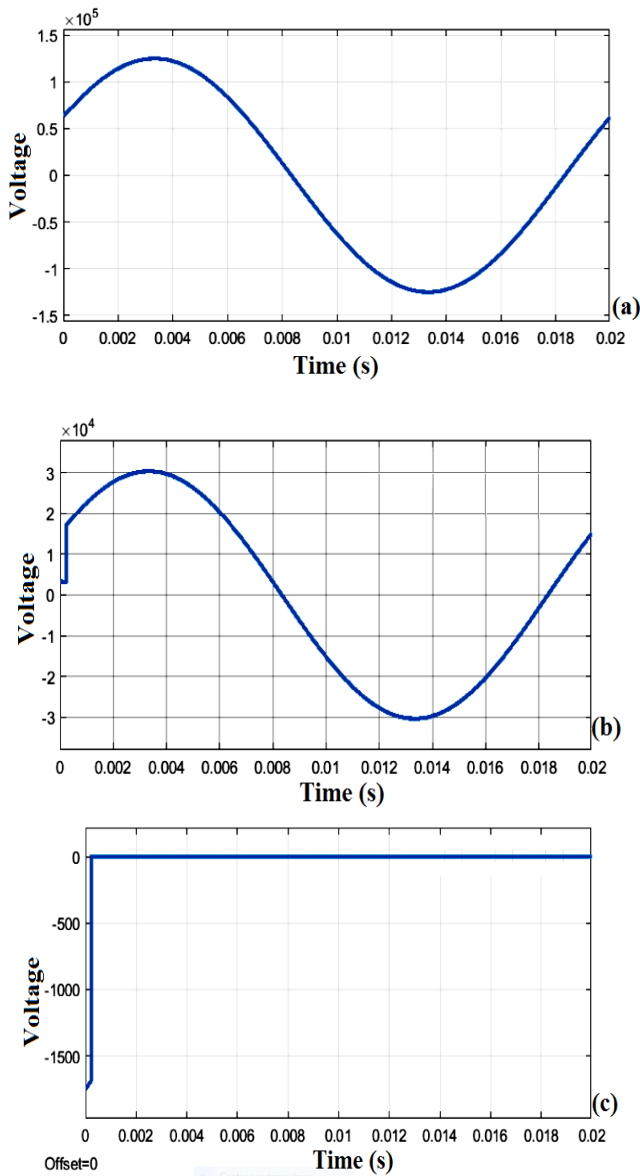
Figure 12 - Crosstalk Curves for z=444.196 ohms and φ=30°: (a) Source Voltage; (b) Near-End Crosstalk; (c) Far-End Crosstalk.
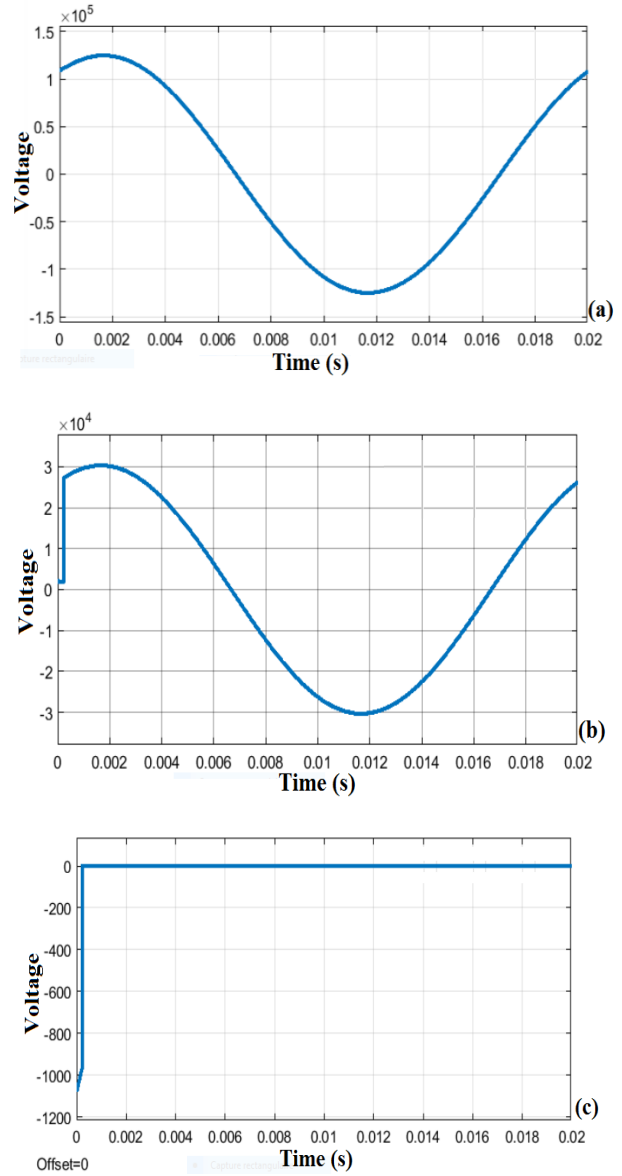

Figure 13 - Crosstalk Curves for z=444.196 ohms and φ=60° : (a) Source Voltage; (b) Near-End Crosstalk; (c) Far-End Crosstalk.

D. Impact of the Impedance on the Crosstalk Phenomenon

a. Crosstalk Phenomenon with Zc=444.196 ohms and φ=15°.

The phase shift is maintained at φ=15° and the impedance is modified from Zc=147.1874 ohms to Zc=444.196 ohms. We obtain Fig. (11). Compared to Fig. (7), the source voltage begins the propagation at 0.5×10^5 v as seen in Fig. 11(a). The introduction of the near-end crosstalk induces a small fluctuation at the beginning of the propagation. Besides, the time of apparition of this fluctuation has decreased from 0.5×10^{-3} s to 0.1×10^{-3} s as depicted in Figs. 7(b) and 11(b). Further, the curve presents a linear and constant behavior at 0.3×10^4 v when $0 < T < 0.1 \times 10^{-3}$ s as seen in Fig. 11(b). The curve undergoes a small vertical and constant behavior from 0.3×10^4 v to 1.00×10^4 v when $T = 0.1 \times 10^{-3}$ s as illustrated in Fig. 11(b).

The curve maintains its sinusoidal form when $T > 0.1 \times 10^{-3}$ s as seen in Fig. 11(b). The introduction of the far-end crosstalk induces the huge broken structure depicted in Fig. 11(c). Besides, the voltage curve exhibits a small ascendant and linear behavior from -1800 v to -1750 v when $0 < T < 0.1 \times 10^{-3}$ s. This behavior changes from ascendant and linear to vertical and constant when $T = 0.1 \times 10^{-3}$ s as illustrated in Fig. 11(c). Moreover, the vertical and constant behavior of the voltage increases from -1750 v to 0 v as depicted in Fig. 11(c). Furthermore, the voltage behavior changes again from the vertical and constant to horizontal and constant when $T > 0.1 \times 10^{-3}$ s as seen in Fig. 11(c). It appears that the far-end crosstalk is closed to 0 v for a long period as seen in Fig 11(c) compared to what is seen in Figs. 7(c), 9(c) and 10(c). The period of action of the crosstalk phenomenon has significantly decreases.
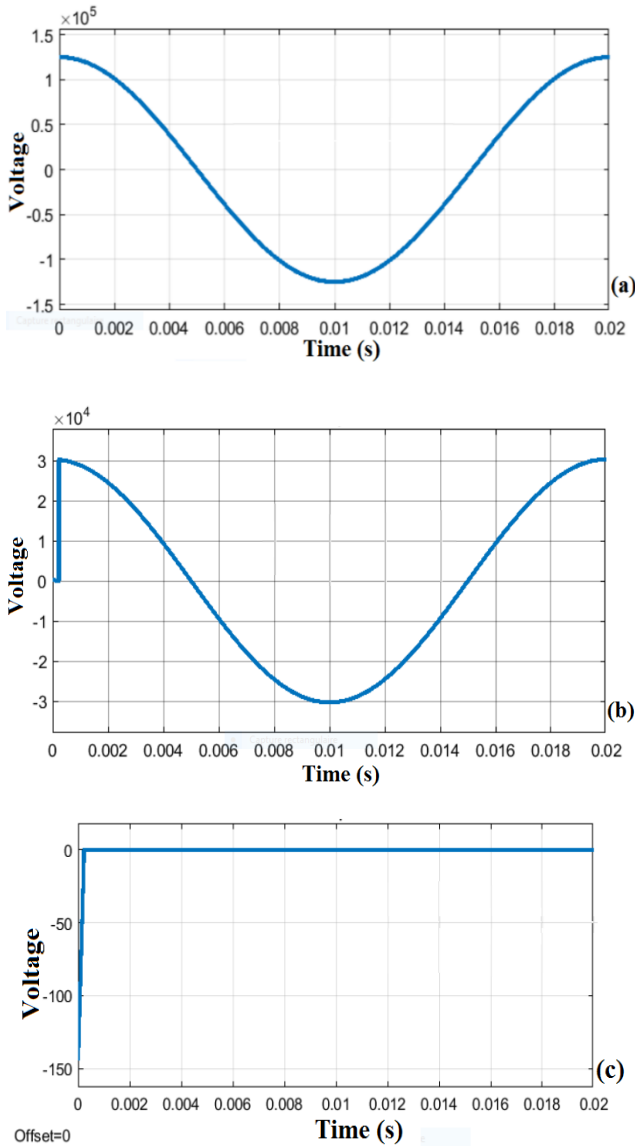
Figure 14 - Crosstalk Curves for z=444.196 ohms and φ=90°: (a) Source Voltage; (b) Near-End Crosstalk; (c) Far-End Crosstalk.

b.   Crosstalk Phenomenon with Zc=444.196 ohms and φ=30°.

The impedance is maintained at Zc=444.196 ohms and the phase shift is increases from φ=15° to φ=30°. Then, we obtain Fig. (12). The source voltage is safeguarded as depicted in Figs. 11(a) and 12(a). The introduction of the near-end crosstalk generates a huge fluctuation at the beginning of the propagation. Besides, the time of apparition of this fluctuation is maintained to T=0.1×10⁻³ s as depicted in Fig. 12(b). Further, the curve shows a very small linear and constant behavior at 0.3×10^4 v when $0 < T < 0.1 \times 10^{-3}$ s as seen in Fig. 12(b). Thereafter, the voltage curve exhibits a long vertical and constant behavior from 0.3×10^4 v to 1.80×10^4 v when $T = 0.1 \times 10^{-3}$ s as illustrated in Fig. 12(b). This fluctuation is different to that illustrated in Fig. 11(b). More so, the curve safeguards its sinusoidal form when $T > 0.1 \times 10^{-3}$ s as seen in Fig. 12(b).

The introduction of the far-end crosstalk provokes the generation of a huge broken structure depicted in Fig. 12(c) similar to that illustrated in Fig. 11(c). After, the voltage curve exhibits a very small ascendant and linear behavior from -1750 v to -1700 v when $0 < T < 0.1 \times 10^{-3}$ s. This behavior

changes from ascendant and linear to vertical and constant when $T = 0.1 \times 10^{-3}$ s as illustrated in Fig. 12(c). In addition, the vertical and constant behavior of the voltage curve increases from -1700 v to 0 v as depicted in Fig. 12(c). Further, the voltage behavior is modified again from the vertical and constant to horizontal and constant when $T > 0.1 \times 10^{-3}$ s as seen in Fig. 12(c). It appears that the far-end crosstalk is closed to 0 v for a long period as seen in Fig 12(c). This behavior is similar to that illustrated in Fig. 11(c).

c.   Crosstalk phenomenon with Zc=444.196 ohms and φ=60°.

The impedance is fixed at Zc=444.196 ohms and the phase shift increases from φ=30° to φ=60°. Then, we obtain Fig. (13). The sinusoidal form of the source voltage is safeguarded as depicted in Fig. 13(a). The introduction of the near-end crosstalk generates a huge fluctuation at the beginning of the propagation. Besides, the time of apparition of this fluctuation is maintained to T=0.1×10⁻³ s as depicted in Fig. 13(b). More so, the curve exhibits a very small linear and constant behavior at 0.1×10^4 v when $0 < T < 0.1 \times 10^{-3}$ s as seen in Fig. 13(b). After, the voltage curve exhibits a long vertical and constant behavior from 0.1×10^4 v to 2.80×10^4 v when $T = 0.1 \times 10^{-3}$ s as illustrated in Fig. 13(b). This fluctuation is most longer compared to that seen in Fig. 12(b). More so, the curve safeguards its sinusoidal form when $T > 0.1 \times 10^{-3}$ s as seen in Fig. 12(b).

The introduction of the far-end crosstalk generates a huge broken structure depicted in Fig. 13(c) similar to that illustrated in Fig. 12(c). Besides, the near-end crosstalk curve exhibits a very small ascendant and linear behavior from -1050 v to -990 v when $0 < T < 0.1 \times 10^{-3}$ s. This behavior is modified from ascendant and linear to vertical and constant when $T = 0.1 \times 10^{-3}$ s as shown in Fig. 13(c). More so, the vertical and constant behavior of the voltage curve increases from -990 v to 0 v as shown in Fig. 13(c). Furthermore, the voltage behavior is modified again from the vertical and constant to horizontal and constant when $T > 0.1 \times 10^{-3}$ s as seen in Fig. 13(c). It clearly appears that the far-end crosstalk is closed to 0 v for a long period as seen in Fig 13(c). This behavior is similar to that illustrated in Fig. 12(c).

d.   Crosstalk Phenomenon with Zc=444.196 ohms and φ=90°.

The impedance is fixed at Zc=444.196 ohms and the phase shift increases from φ=60° to φ=90°. Hence, we obtain Fig. (14). The sinusoidal form of the source voltage is safeguarded as depicted in Fig. 14(a). The introduction of the near-end crosstalk generates a huge fluctuation at the beginning of the propagation. Besides, the time of apparition of this fluctuation is maintained to T=0.1×10⁻³ s as depicted in Fig. 14(b).
Moreover, the curve exhibits a very small linear and constant behavior at 0 v when $0 < T < 0.1 \times 10^{-3}$ s as seen in Fig. 14(b). In addition, the voltage curve shows a long vertical and constant behavior which varies from 0 v to 3.00×10^4 v when $T = 0.1 \times 10^{-3}$ s as presented in Fig. 14(b). This fluctuation is most longer compared to that seen in Fig. 13(b).

8

Further, the curve safeguards its sinusoidal form when $T>0.1\times10^{-3}$ s as seen in Fig. 14(b).

The introduction of the far-end crosstalk generates a huge broken structure depicted in Fig. 14(c) similar to that illustrated in Fig. 13(c). More so, the near-end crosstalk curve exhibits a gradual ascendant behavior which varies from -140 v to 0 v when $0<T<0.1\times10^{-3}$ s as seen in Fig. 14(c). This behavior is modified from gradual ascendant to horizontal and constant behavior when $T>0.1\times10^{-3}$ s as shown in Fig. 14(c). Furthermore, horizontal and constant behaviors of the voltage curve are closed to 0 v for a long period as shown in Fig. 14(c). Besides, this behavior is different to that illustrated in Fig. 14(c). It appears that the far-end crosstalk significantly decreases as the phase shift increases.

E. Discussion

a. Crosstalk Values' Presentation

Some crosstalk voltage values coming from all the aforementioned figures are listed in Table 3.

Table 3- Results Obtained with Two Types of Lines

Z_C= 147.1874 ohms			
Near-End crosstalk	Far-End crosstalk	Phase shift (°)	Reduction rate
10 KV	0.50 KV	15	
9.5 KV	0.50 KV	30	
27 KV	0.32 KV	60	
10 KV	0.50 KV	90	
Zc=444.1967 ohms			
Near-End - crosstalk	Far-End - crosstalk	Phase shift (°)	Reduction rate
10 KV	-1.80 KV	15	
18 KV	-1.75 KV	30	**100%**
28 KV	-1.05 KV	60	
30 KV	-0.14 KV	90	

All the negative values of far-end crosstalk are directly related to 0 v. Consequently, the reduction rate of crosstalk is considered to be 100% as seen in Table 3.

b. Analysis and Comparison of Results

Previous results in literature				
Methods	Near-end crosstalk	Far-end crosstalk	Limits	Observations
Adapted terminations [21]	860mV	150mV	Increases the signal to crosstalk ratio	Zc1=147.2 Ω
Pseudo-adapted endings[21]	80mV	40mV	Does not completely eliminate	Zc1=147.2 Ω
	1000mV	200mV		
Our results for the contribution				
Pseudo-adapted endings	7.8588 kV	0V		Zc1=147.2 Ω zero crosstalk
	9.38kV	0V		Zc2=444.196Ω zero crosstalk

IV. CONCLUSION

We model the line through telegraphers' equations. Then, we use Pseud-matched impedances' method to reduce the crosstalk phenomenon in the line (victim driver). Some interesting results related to the values and the physical impact of the crosstalk phenomenon during the propagation

following two cases. Case 1 : Zc=147.1874 ohms and φ (15° ; 30° ; 60° ; 90°). (i) The source voltage exhibits a sinusoidal form. (ii) The near-end crosstalk generates a small broken point (small fluctuation) at the beginning of the propagation. As the phase shift increases, we note the following points. This small fluctuation is changed to a huge fluctuation. The source voltage form is modified from the sinusoidal to the linear. Thereafter, this sinusoidal form is also transformed from linear to sinusoidal associated with a big broken point. Similar behavior are obtained for different values of the phase shift (φ=15° and φ=90°). (iii) The far-end crosstalk induces a huge broken point (huge broken fluctuation). Then, the sinusoidal form of the source voltage is transformed into a huge broken fluctuation. The general aspect of this huge broken fluctuation is maintained as the phase shift increases. (iv) The crosstalk phenomenon decreases the voltage values during the propagation. The far-end crosstalk presents the lower voltage values compared to the near-end crosstalk. (v) The cancellation time of crosstalk phenomenon is T=0.6 ms. Case 2 : Zc=444.196 ohms and φ (15° ; 30° ; 60° ; 90°). (i) The near-end crosstalk generates a small broken point (small fluctuation) which increases as the phase shift increases. The voltage curve exhibits a fluctuation associated with sinusoidal form. (ii) The far-end crosstalk induces an opposite huge broken fluctuation compared to the that obtained in the first case. (iii) The cancellation time of the crosstalk phenomenon is decreased from T=0.6 ms to T=0.1 ms.

DECLARATION STATEMENT

Funding/ Grants/ Financial Support	No, I did not receive.
Conflicts of Interest/ Competing Interests	No conflicts of interest to the best of our knowledge.
Ethical Approval and Consent to Participate	No, the article does not require ethical approval and consent to participate with evidence.
Availability of Data and Material/ Data Access Statement	Not relevant.
Authors Contributions	All authors have equal participation in this article.

Crosstalk Characterization and Reduction in Power Lines

REFERENCES

1. Chunming Qiao, Member, ZEEE, Rami Georges Melhem, Donald M. Chiarulli, and Steven P. Levitan, 'A Time Domain Approach for Avoiding Crosstalk in Optical Blocking Multistage Interconnection Networks. JOURNAL OF LIGHTWAVE TECHNOLOGY, VOL. 12, NO. 10, OCTOBER 1994. https://doi.org/10.1109/50.337500
2. Yunfeng Shen, Kejie Lu, and Wanyi Gu, Coherent and Incoherent Crosstalk Coherent and Incoherent Crosstalk in WDM Optical Networks. JOURNAL OF LIGHTWAVE TECHNOLOGY, VOL. 17, NO. 5, MAY 1999 https://doi.org/10.1109/50.762889
3. Faten Sahel, Pascal Guilbault, Farouk Vallette, Sylvain Feruglio. A Crosstalk Modelling Method between a Power Supply and a Nearby Signal in High-density Interconnection PCBs. 2021 22nd International Symposium on Quality Electronic Design (ISQED), Apr 2021, Santa Clara, CA, United States. pp.227-232, ff10.1109/ISQED51717.2021.9424304ff. ffhal-03225181ff . https://doi.org/10.1109/ISQED51717.2021.9424304
4. Rza Bashirov *, Tolgay Karanfiller, On path dependent loss and switch crosstalk reduction in optical networks. Information Sciences 180 (2010) 1040–1050. https://doi.org/10.1016/j.ins.2009.11.017
5. Isaak E. Müller, Jacob R. Rubens, Tomi Jun, Daniel Graham, Ramnik Xavier and Timothy K. Lu, Gene networks that compensate for crosstalk with crosstalk. NATURE COMMUNICATIONS (2019) 10:4028 | https://doi.org/10.1038/s41467-019-12021-y https://doi.org/10.1038/s41467-019-12021-y
6. E. L. Goldstein, L. Eskildsen, and A. F. Elrefaie, "Performance implications of component crosstalk in transparent lightwave networks," IEEE Photon. Technol. Lett., vol. 6, pp. 657–660, May 1994. https://doi.org/10.1109/68.285571
7. C. S. Li and F. Tong, "Crosstalk and interference penalty in all-optical networks using static wavelength routers," J. Lightwave Technol., vol. 14, pp. 1120–1126, June 1996. https://doi.org/10.1109/50.511613
8. H. Takahashi, K. Oda, and H. Toba, "Impact of crosstalk in an arrayedwaveguide multiplexer on N N optical interconnection," J. Lightwave Technol., vol. 14, pp. 1097–1105, June 1996. https://doi.org/10.1109/50.511611
9. M.M. Vaez, C.T. Lea, Strictly nonblocking directional-coupler based switching networks under crosstalk constraint, IEEE Transactions on Communication 48 (2000) 316–323. https://doi.org/10.1109/26.823564
10. A.K. Katangur, S. Akkaladevi, Y. Pan, Analyzing the performance of optical multistage interconnection networks with limited crosstalk, Cluster Computing 10 (2007) 241–250 https://doi.org/10.1007/s10586-007-0018-7
11. X. Jiang, H. Sheng, M.R. Khandker, S. Horiguchi, Blocking behaviors of crosstalk-free optical banyan networks on vertical stacking, IEEE/ACM Transactions on Networking 11 (2003) 982–993. https://doi.org/10.1109/TNET.2003.820425
12. Rowland, M. A. & Deeds, E. J. Crosstalk and the evolution of specificity in two-component signaling. Proc. Natl Acad. Sci. USA 111, 5550–5555 (2014). https://doi.org/10.1073/pnas.1317178111
13. S. D. Dods, J. P. R. Lacey, and R. S. Tucker, "Homodyne crosstalk in WDM ring and bus networks," IEEE Photon. Technol. Lett., vol. 9, pp. 1285–1287, Sept. 1997. https://doi.org/10.1109/68.618506
14. Rhodius, V. A. et al. Design of orthogonal genetic switches based on a crosstalk map of σs, anti-σs, and promoters. Mol. Syst. Biol. 9, 702 (2013). https://doi.org/10.1038/msb.2013.58
15. Capra, E. J., Perchuk, B. S., Skerker, J. M. & Laub, M. T. Adaptive mutations that prevent crosstalk enable the expansion of paralogous signaling protein families. Cell 150, 222–232 (2012) https://doi.org/10.1016/j.cell.2012.05.033
16. Guo, X. & Wang, X. F. Signaling cross-talk between TGF-β/BMP and other pathways. Cell. Res. 19, 71–88 (2009). https://doi.org/10.1038/cr.2008.302
17. Vert, G. & Chory, J. Crosstalk in cellular signaling: background noise or the real thing? Dev. Cell 21, 985–991 (2011) https://doi.org/10.1016/j.devcel.2011.11.006
18. Wu, F., Menn, D. J. & Wang, X. Quorum-sensing crosstalk-driven synthetic circuits : from unimodality to trimodality. Chem. Biol. 21, 1629–1638 (2014). https://doi.org/10.1016/j.chembiol.2014.10.008
19. Morey, K. J. et al. Crosstalk between endogenous and synthetic components - synthetic signaling meets endogenous components. Biotechnol. J. 7, 846–855 (2012). https://doi.org/10.1002/biot.201100487
20. T. Ditchi. "les lignes de transmission". Course on transmission lines. University of SORBONNE, page 1-74, (2015).
21. S. Roblot. "Caractérisation des couplages électromagnétiques dans les réseaux filaires cuivre en vue d'optimiser les transmissions à haut débit". Dotorate thesis of University of Limoges. 1-164, (2007).
22. M. Kachout, "Interference reduction for RF signal integrity". 1-118, (2016).
23. F. Broydé, "Radically eliminating crosstalk in interconnections" Electronique, No.140, pp. 57-61, 2003.

AUTHOR PROFILE

Dr. Jacquie Therese NGO BISSE, Laboratory of Electrotechnics, Automatics and Energy, Department of Maintenance, Higher Technical Teachers Training College (HTTTC) of EBOLOWA, University of EBOLOWA, P.O. Box 886, Ebolowa, Cameroon. Jacquie Therese Ngo Bisse is a specialist in Electronic Systems and maintenance. She is a Ph.D. holder from the University of Douala. She is currently an Associate Lecturer with the Higher Technical Teacher's Training College of Ebolowa associated to University of EBOLOWA in Cameroun. His research is linked to Electronic systems, and Power Systems Modeling.

Dr. Bedel Giscard ONANA ESSAMA, Laboratory of Electrotechnics, Automatics and Energy, Department of Electrical Engineering, Higher Technical Teachers Training College (HTTTC) of EBOLOWA, University of EBOLOWA, P.O. Box 886, Ebolowa, Cameroon. Bedel Giscard Onana Essama is a specialist in Energy-Electric and Electronic Systems. He is a Ph.D. holder from the University of Yaounde 1. He is currently an Associate Lecturer with the Higher Technical Teacher's Training College of Ebolowa associated to University of EBOLOWA in Cameroun. His research is linked to Energetic systems, Power Systems Modeling, Complex Systems modeling, Nonlinear Dynamics, Optical fiber and Medical Physics.

Dr. Joseph KOKO KOKO, Laboratory of Electrotechnics, Automatics and Energy, Department of Electrical Engineering, Higher Technical Teachers Training College (HTTTC) of EBOLOWA, University of EBOLOWA, P.O. Box 886, Ebolowa, Cameroon. Joseph KOKO KOKO is a specialist in Energic systems and power lines. He is a Ph.D. holder from the University of Douala. He is currently worked with the Higher Technical Teacher's Training College of Ebolowa associated to University of EBOLOWA in Cameroun. His research is linked to Power systems and Power Electronics.

Professor Jacques ATANGANA, Laboratory of Electronics, Electrotechnics and Automatics, Department of Physics, Higher Teachers Training College (HTTC) of Yaoundé, University of Yaoundé 1, P.O. Box 47, Yaoundé, Cameroon. Jacques Atangan is a specialist in electronic systems. He is a Ph.D. holder from the University of Yaoundé 1. He is currently a Professor with the Higher Teacher's Training College of Yaoundé associated to University of Yaoundé 1 in Cameroun. His research is related to Electrical transmission lines and the complex systems modeling.

Professor Salome NDJAKOMO ESSIANE, Laboratory of Electrotechnics, Automatics and Energy, Department of Electrical Engineering, Higher Technical Teachers Training College (HTTTC) of EBOLOWA, University of EBOLOWA, P.O. Box 886, Ebolowa, Cameroon. Salomé Ndjakomo Essiane is a specialist in electronics and optoelectronics. She is a Ph.D. holder from the IBN to fail Morocco University. She is currently a Professor with the Higher Technical Teacher's Training College of Ebolowa associated to University of EBOLOWA in Cameroun. Her research is related to Electrical power engineering and power systems modeling.
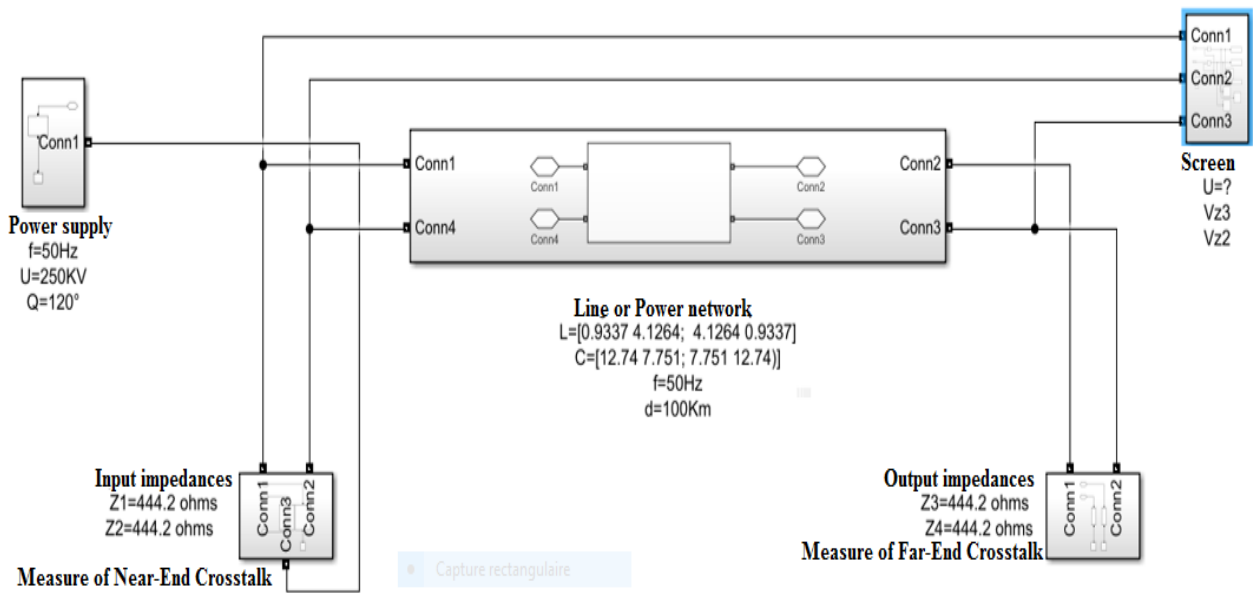
APPENDIX
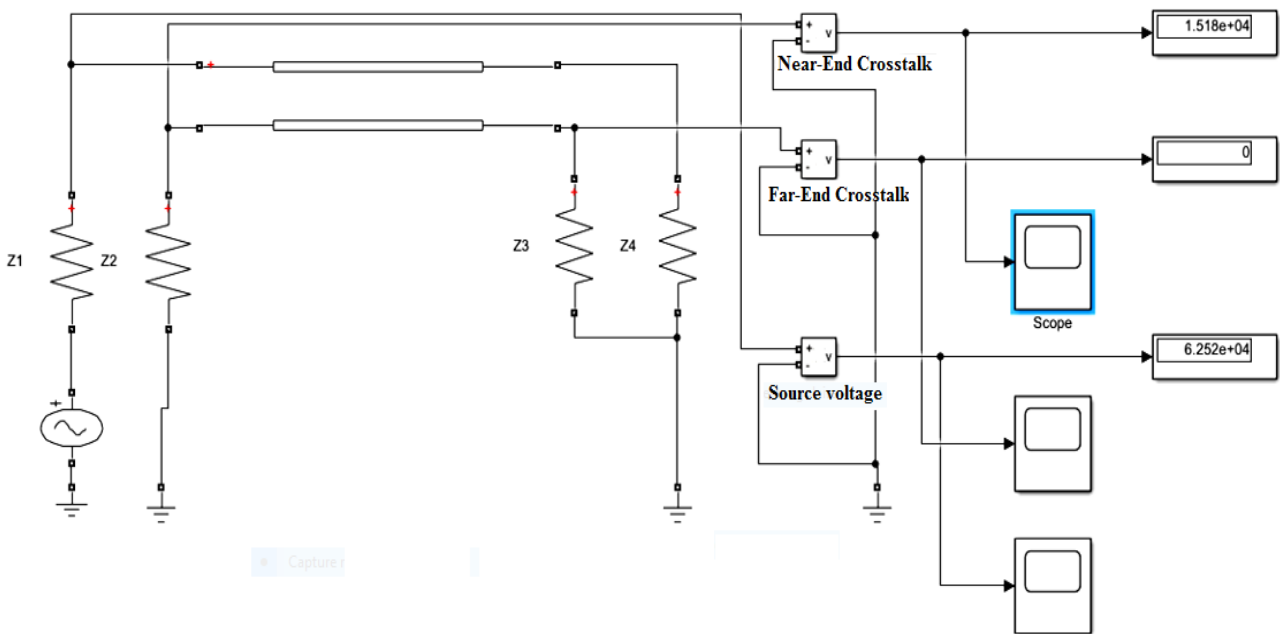A.1.

Fig. 4. Simulink Diagram of the Power Network

Fig. 6. Internal Parameters of the Power Network